doi:10.1006/jmbi.2001.5084 available online at http://www.idealibrary.com on IDEAL® *J. Mol. Biol.* (2001) **313**, 1127–1138

JMB

Crystal Structure of the Liganded SCP-2-like Domain of Human Peroxisomal Multifunctional Enzyme Type 2 at 1.75 Å Resolution

Antti M. Haapalainen[1], Daan M. F. van Aalten[2], Gitte Meriläinen[1] Jorma E. Jalonen[3], Päivi Pirilä[1], Rik K. Wierenga[1], J. Kalervo Hiltunen[1] and Tuomo Glumoff[1]*

[1]*Biocenter Oulu and Department of Biochemistry University of Oulu, P.O. Box 3000, FIN-90014, University of Oulu, Finland*

[2]*Wellcome Trust Biocentre, School of Life Sciences University of Dundee, Dundee DD1 5EH, UK*

[3]*Department of Chemistry University of Oulu, P.O. Box 3000, FIN-90014, University of Oulu, Finland*

**Corresponding author*

β-Oxidation of amino acyl coenzyme A (acyl-CoA) species in mammalian peroxisomes can occur *via* either multifunctional enzyme type 1 (MFE-1) or type 2 (MFE-2), both of which catalyze the hydration of *trans*-2-enoyl-CoA and the dehydrogenation of 3-hydroxyacyl-CoA, but with opposite chiral specificity. MFE-2 has a modular organization of three domains. The function of the C-terminal domain of the mammalian MFE-2, which shows similarity with sterol carrier protein type 2 (SCP-2), is unclear. Here, the structure of the SCP-2-like domain comprising amino acid residues 618-736 of human MFE-2 (dΔhΔSCP-2L) was solved at 1.75 Å resolution in complex with Triton X-100, an analog of a lipid molecule. This is the first reported structure of an MFE-2 domain. The dΔhΔSCP-2L has an α/β-fold consisting of five β-strands and five α-helices; the overall architecture resembles the rabbit and human SCP-2 structures. However, the structure of dΔhΔSCP-2L shows a hydrophobic tunnel that traverses the protein, which is occupied by an ordered Triton X-100 molecule. The tunnel is large enough to accommodate molecules such as straight-chain and branched-chain fatty acyl-CoAs and bile acid intermediates. Large empty apolar cavities are observed near the exit of the tunnel and between the helices C and D. In addition, the C-terminal peroxisomal targeting signal is ordered in the structure and solvent-exposed, which is not the case with unliganded rabbit SCP-2, supporting the hypothesis of a ligand-assisted targeting mechanism.

Keywords: multifunctional enzyme; β-oxidation; peroxisome; Triton X-100; sterol

Introduction

All the characterized β-oxidation pathways are found to have a multifunctional enzyme (MFE). A common feature of these MFEs is that they catalyze the second and the third reaction of the pathway. The properties of the MFEs, like subunit composition and associated enzymatic activities, vary depending on species and whether they originate from mitochondria, peroxisomes (eukaryotes) or from the cytoplasm (bacteria).[1] Multifunctional enzyme type 2 (MFE-2, EC 1.1.1.62) in mammals, also known as D-bifunctional protein"[2] and 17β-hydroxysteroid dehydrogenase type 4 (17β-HSD 4),[3] metabolizes *trans*-2-enoyl-CoA esters to 3-keto compounds *via* (3*R*)-hydroxyacyl-CoA intermediates in the peroxisomal β-oxidation. MFE-2 has been cloned and characterized from a wide range of organisms.[4–8] Analysis of accumulating metabolites in patients with MFE-2 deficiency and ''knock-out'' mice, together with enzymatic properties observed *in vitro*, suggest that the physiological

Abbreviations used: MFE, multifunctional enzyme; MFE-2, multifunctional enzyme type 2; dΔhΔSCP-2L, MFE-2 truncated for (3*R*)-hydroxyacyl-CoA dehydrogenase and *trans*-2-enoyl-CoA hydratase 2 domains; SCP-2L, sterol carrier protein type 2-like domain; SCP-2, sterol carrier protein type 2; SCPX, sterol carrier protein x; C6, fatty acid molecule with six carbon atoms; CoA, coenzyme A; PTS1, peroxisomal targeting signal type 1; SDS-PAGE, sodium dodecyl sulfate-polyacrylamide gel electrophoresis.

E-mail address of the corresponding author: Tuomo.Glumoff@oulu.fi

0022-2836/01/051127–12 $35.00/0

role of mammalian MFE-2 is the peroxisomal β-oxidation of very-long-chain fatty acids and 2-methyl-branched-chain fatty acids as well as di- and trihydroxycholestanoic acids.[9,10] (*3R*)-hydroxyacyl-CoA dehydrogenase, which catalyzes the third reaction of the β-oxidation pathway, is located to the N terminus of MFE-2, followed by the *trans*-2-enoyl-CoA hydratase 2 domain, responsible for the second reaction. Both domains were first identified experimentally in yeast MFE-2.[11] Subsequently, amino acid sequence comparisons and *in vitro* enzymatic characterization have revealed that mammalian MFE-2s have the same domain order.[6–8,12] However, the hydratase 2 domain in mammalian MFE-2s is followed by a sterol carrier protein type 2 like domain (SCP-2L), which is absent in the yeast proteins.

In addition to mammalian MFE-2, SCP-2 or SCP-2L are found in SCPX proteins (sterol carrier protein x, also known as non-specific lipid transfer protein; ns-LTP), *Caenorhabditis elegans* behavioral protein (unc-24),[13] PXP-18 (oleate-induced peroxisomal protein POX18)[14] and human SLP-1 (stomatin-like protein).[15] The C-terminal domain of human MFE-2, which carries the C-terminal peroxisomal targeting signal type one[16,"17] (PTS1), reveals 40 % amino acid sequence identity with the human SCP-2 and the C-terminal domain of the human SCPX.[8,18] SCP-2 and SCPX are encoded by the same gene and they arise *via* alternate initiation of translation. In the longer variant (SCPX), the 3-ketoacyl-CoA thiolase domain precedes the SCP-2 domain. The SCP-2L of MFE-2 and SCP-2/SCPX are encoded by gene regions with similar intron-exon structure, suggesting that these multidomain proteins have acquired the SCP-2 or SCP-2L by fusing genetic material from the same origin.[9,18,19]

Mice lacking SCP-2/SCPX developed a peroxisomal β-oxidation deficiency-like phenotype,[20] supporting the suggestion that SCP-2/SCPX function as carriers for fatty acyl-CoAs rather than for sterols as initially anticipated.[21,22] In addition, SCP-2 was shown to interact with acyl-CoA oxidase,[23] suggesting that SCP-2 may function in the transfer of fatty acyl-CoA derivatives to acyl-CoA oxidase. Except for the demonstration that the activity of (*3R*)-hydroxyacyl-CoA dehydrogenase of porcine MFE-2 towards steroids and fatty acyl-CoAs is not changed upon ablating the SCP-2L,[8] there exists no published data addressing the physiological function of the SCP-2L in MFE-2.

Our long-term aim is to elucidate the structure-function relationship of MFE-2. As a part of that project we have crystallized the C-terminal region of human peroxisomal MFE-2, and report here its liganded crystal structure. The recombinant C-terminal region contained SCP-2L but not (*3R*)-hydroxyacyl-CoA dehydrogenase and *trans*-2-enoyl-CoA hydratase 2 domains; subsequently it is referred as dΔhΔSCP-2L. The structure shows a hydrophobic tunnel occupied by the ligand, a feature not present in the previously published unliganded rabbit SCP-2 crystal structure[24] and unliganded human SCP-2 NMR structure.[25]

Results

Identification and crystallization of SCP-2L of human MFE-2

Multiple amino acid sequence alignments of MFE-2s were used to identify the C-terminal SCP-2L (data not shown). In addition, the amino acid sequence alignment of the SCP-2L of human MFE-2 with all known eukaryotic SCP-2 or SCP-2L proteins found in PSI-BLAST[26] shows 21 % amino acid sequence similarity (Figure 1) as specified by CLUSTAL W [27] using gonnet matrix. Subsequently, the fragment, Glu618-Leu736, of the human MFE-2 (dΔhΔSCP-2L) was expressed in *Escherichia coli* and purified using anion, cation and size-exclusion chromatographies to apparent homogeneity as demonstrated by SDS-polyacrylamide gel electrophoresis. The peak obtained with MALDI-TOF mass spectrometric analysis gave a mass value of 13,244.49 g/mol, which corresponded to the calculated mass of the protein (13,244.47 g/mol). The purified dΔhΔSCP-2L was crystallized and a data set was collected from a frozen crystal using synchrotron radiation. The liganded structure of dΔhΔSCP-2L was solved at 1.75 Å resolution applying molecular replacement techniques.

Description of the structure

The dΔhΔSCP-2L has an α/β-fold composing of five α-helices and five β-strands (Figure 2). The overall dimensions of the dΔhΔSCP-2L are 39 Å × 32 Å × 32 Å and thus its shape is more spherical than that reported for the rabbit SCP-2 (40 Å × 25 Å × 25 Å).[24] The core of the protein is formed by five β-strands with the mixed sheet structure of −1, −1, +3X, +1 topology. Strand I is formed by residues Ala32-Lys40, strand II by Asn43-Leu52, strand III by Lys58-Gly62, strand IV by Asp69-Ser75, and strand V by Lys99-Asn103. The solvent-exposed side of the β-sheet layer is mainly populated by polar residues, while the side, which is facing the interior of the protein, is mainly composed of hydrophobic amino acids. Interestingly, the crossover loop region, which connects strands III and IV (Figure 1), is almost completely formed by non-polar and uncharged amino acids, even though this loop is facing the solvent. In the rabbit SCP-2 the same loop is formed by polar residues: Asn487, Ser488, Asp489, Lys490, Lys491, Ala492 and Asp493.

The β-sheet layer is covered on one side by five α-helices (A-E) (Figure 2); three of these helices are short and composed of two turns. Each α-helix is amphipathic, with the polar residues facing the solvent and apolar ones facing the interior of the protein. Helices A (Ser8-Lys20) and B (Pro24-Val30) are connected *via* a short loop of three amino acid residues and they are perpendicular with respect

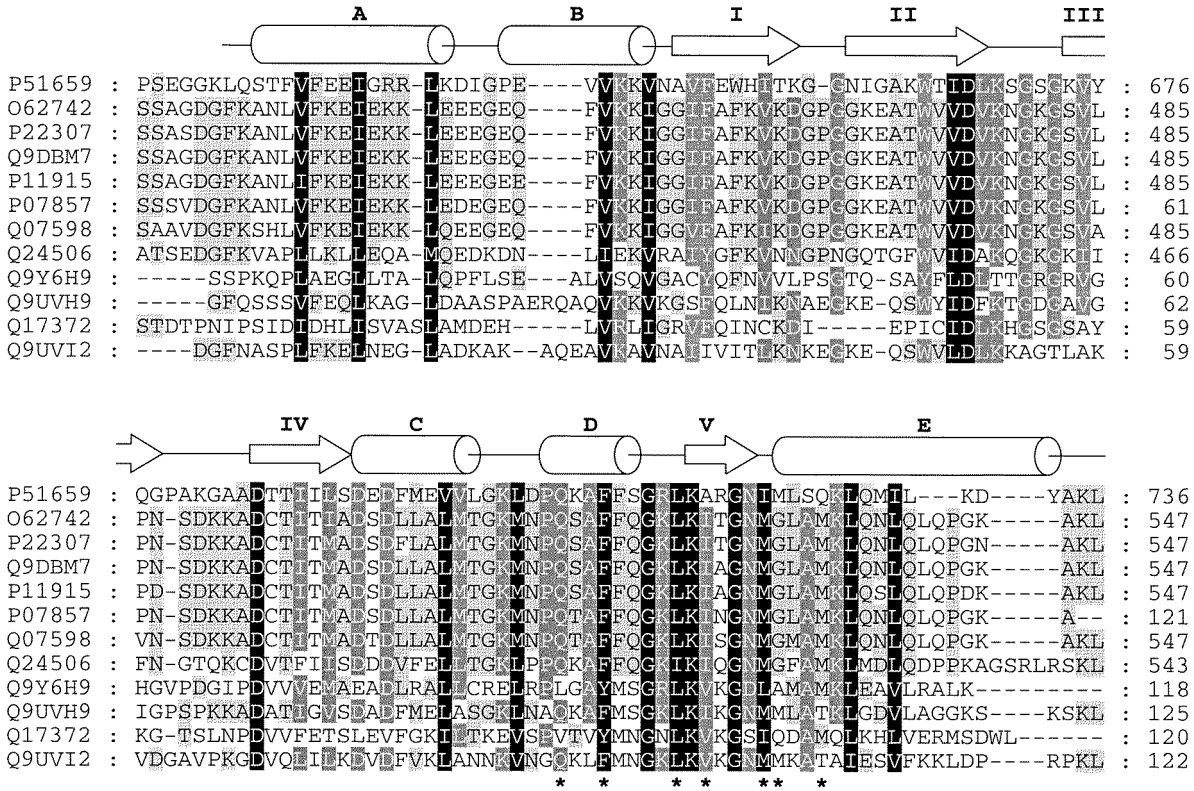

Figure 1. Alignment of the amino acid sequence of the SCP-2L from human MFE-2 with those of other known SCP-2 or SCP-2L proteins from eukaryotes. Apart from SCP-2, which is also expressed as an individual protein, the other homologues are C-terminal domains in multifunctional/domain proteins. The SCP-2L of human MFE-2 (P51659) was aligned with rabbit SCP-2/SCPX (O62742), human non-specific lipid-transfer protein (P22307), mouse SCP-2 (Q9DBM7), rat non-specific lipid-transfer protein (P11915), bovine non-specific lipid-transfer protein (P07857), chicken non-specific lipid-transfer protein (Q07598), fruit-fly SCP-2/SCPX (Q24506), human stomatin-like protein UNC-24 (Q9Y6H9), *Glomus mosseae* FOX2 (Q9UVH9),[27] *Caenorhabditis elegans* UNC-24 (Q17372) and *Candida tropicalis* PXP-18 (Q9UVI2). Alignments were performed using the BESTFIT program (EMBL, Heidelberg). Residues conserved throughout all 12 sequences are shaded black, and the others in regions with a high degree of sequence similarity are either dark gray (80-99 %) or light gray (60-79 %). The secondary structures of dΔhΔSCP-2L, defined by DSSP,[29] are shown. The cylinders indicate α-helices and the arrows indicate β-strands. The amino acid residues marked with asterisk form the entrance of the hydrophobic tunnel in the dΔhΔSCP-2L structure.

to each other. Helices C (Asp76-Leu84) and D (Pro89-Ser95) are also connected *via* a short loop.

The last helix, helix E (Met105-Tyr117), is functionally in a central position, with respect to both ligand binding and the peroxisomal targeting signal, which is located at its C-terminal end. The C-terminal helices are different in all known SCP-2 structures (Figure 3). In our dΔhΔSCP-2L structure this helix comprises almost four full turns with an ordered and solvent-exposed peroxisomal targeting signal (-Ala-Lys-LeuOH), while in the human[25] and rabbit[24] structures the same region is composed of a shorter helix with either the first half of the region or the second half of the region as a random coil, respectively.

In addition to dΔhΔSCP-2L and SCP-2, the structures of three other acyl-CoA binding proteins have been described.[31–33] All of these proteins are α-helical proteins although they are not sequence or structure related. Therefore, the α/β-fold in SCP-2 and SCP-2L proteins is unique and indicates that acyl-CoA binding proteins are not evolutionarily related.

Identification of the ligand in the tunnel

After calculating the first electron density maps, well-defined density was observed for an ordered molecule occupying the hydrophobic ligand-binding cavity. A possible candidate for the difference density inside the protein was Triton X-100, because it was needed for crystallization. Mass spectrometric analysis of the purified protein not exposed to Triton X-100 gave only one peak showing that the recombinant protein was unliganded, whereas the spectrum of the washed dΔhΔSCP-2L crystal was different. Seven peaks with mass differences matching the ethoxy-repeats of the triton molecule could be identified (see Figure 4 for the definition of ethoxy-repeat), pointing to the presence of detergent molecules of varying chain length in the dΔhΔSCP-2L crystal. This agrees with the electron density map where the octylphe-

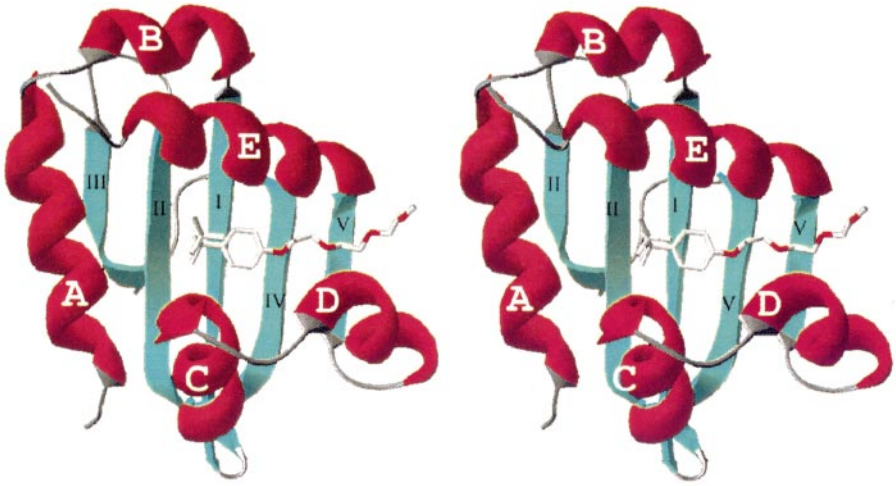

Figure 2. Stereo view of dΔhΔSCP-2L. The structure is drawn as ribbons with helices colored red, β-strands with turquoise and loops gray. The ligand bound to the protein is Triton X-100. The β-strands and α-helices are indicated by roman numerals (I-V) and capitals (A-E), respectively. The Figure was made with Swiss-PdbViewer[30] and Adobe Photoshop.

nol end and three ethoxy-repeats of the triton molecule can be seen (Figure 5), while the tail of the triton molecule that extends into the solvent does not have interpretable electron density. The weak electron-density for the tail indicates differences in tail lengths and possible mobility of the last ethoxy-repeats resulting in higher *B*-factors. According to the manufacturer, Triton X-100 is a heterogeneous product with an average of ten ethoxy-repeats per molecule.

Although Triton X-100 is not a natural ligand for dΔhΔSCP-2L, it could be considered a model molecule for lipids binding to SCP-2 or SCP-2L proteins. In our case, Triton X-100 is positioned in the binding site such that the hydrophobic end lies deep inside the hydrophobic tunnel, while the hydrophilic, ethoxy-repeat, end extends outside of the protein. Apparent K_d values of Triton X-100 and two plausible physiological ligands, palmitoyl-CoA and *trans*-2-hexadecenoyl-CoA, binding to dΔhΔSCP-2L, as estimated with surface plasmon resonance measurements, are 400 μM, 20 μM and 40 μM, respectively.

Hydrophobic tunnel

The dΔhΔSCP-2L described here contains an ordered Triton molecule that defines the ligand-

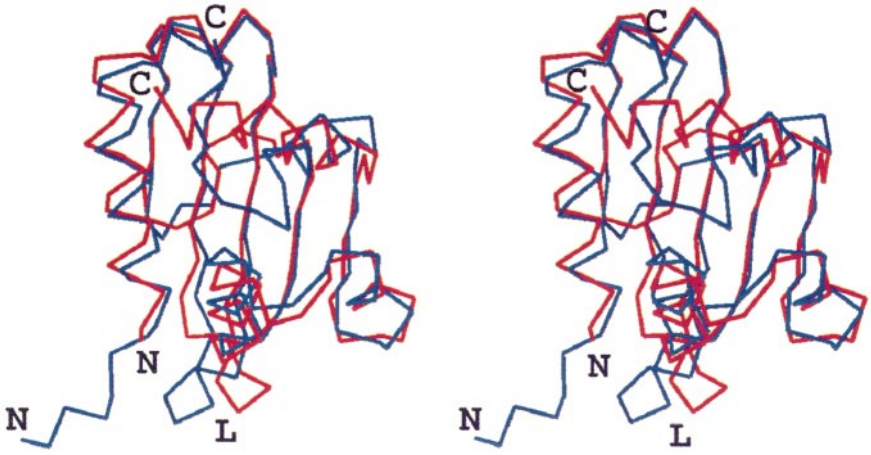

Figure 3. Superimposition of the backbone structures of the unliganded rabbit SCP-2[24] (PDB entry 1c44) and liganded dΔhΔSCP-2L. The rabbit SCP-2 is colored blue and dΔhΔSCP-2L is red. ''N'' and ''C'' indicate the amino and carboxyl terminus, respectively. The two structures align with an overall rms deviation of 1.8 Å, as calculated from all C^{α} atoms. However, in the last C-terminal helix the rms deviation is more than 7 Å. The loop between the β-strands I and II, indicated by ''L'', also has higher rmsd values. The dΔhΔSCP-2L is in the same orientation as that shown in Figure 2.

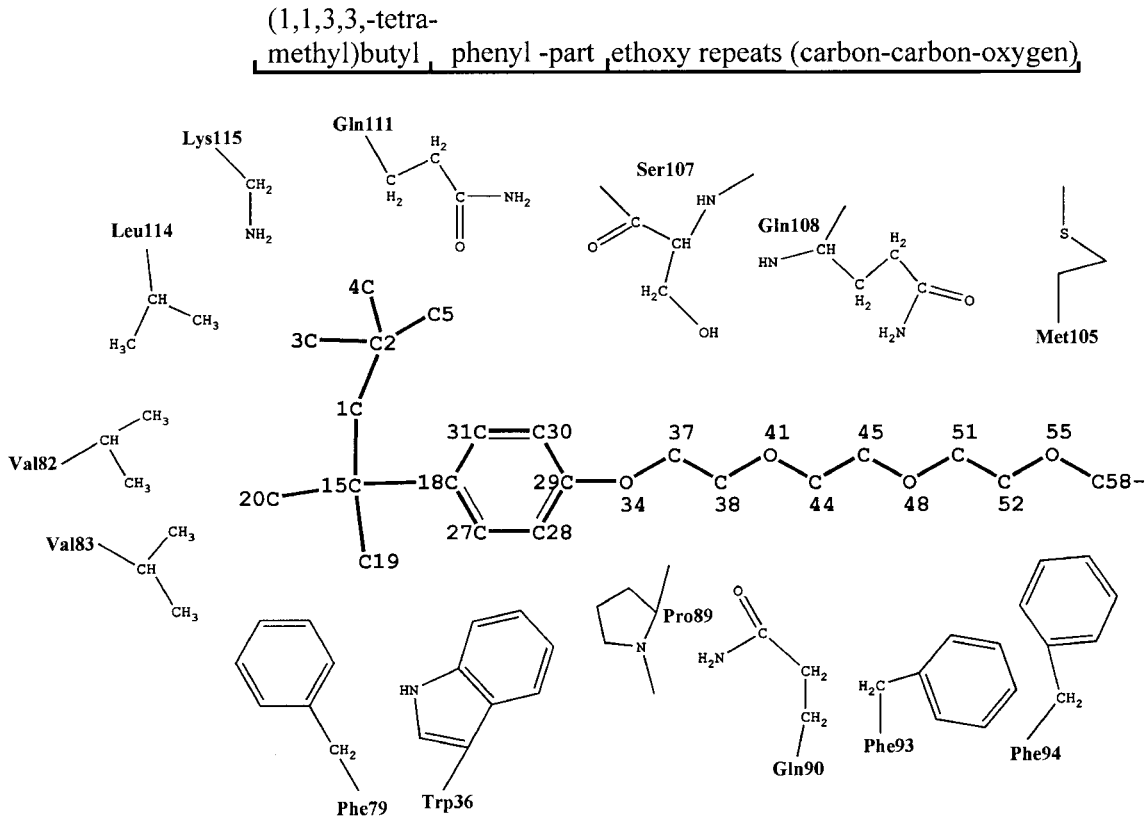

Figure 4. A drawing of the contact environment between the Triton X-100 molecule and dΔhΔSCP-2L. For clarity, the distances are shown in Table 1. Only one hydrogen bond (3.1 Å) is formed between NE2 of Gln108 and O55 of the Triton molecule. Triton X-100 consists of three structural parts: (1,1,3,3-tetramethyl)butyl, phenyl and ethoxy-repeats. The Figure was produced with ChemDraw software.

binding site comprising a hydrophobic tunnel. A hydrophobic tunnel in rabbit and human SCP-2s has been also observed,[24,25] but our structure shows for the first time an ordered ligand occupying this tunnel (Figures 2 and 6). The tunnel, with a diameter of 9 Å and a length of 18 Å, is large enough to accommodate ligands of the size of various fatty acids or their CoA derivatives such as

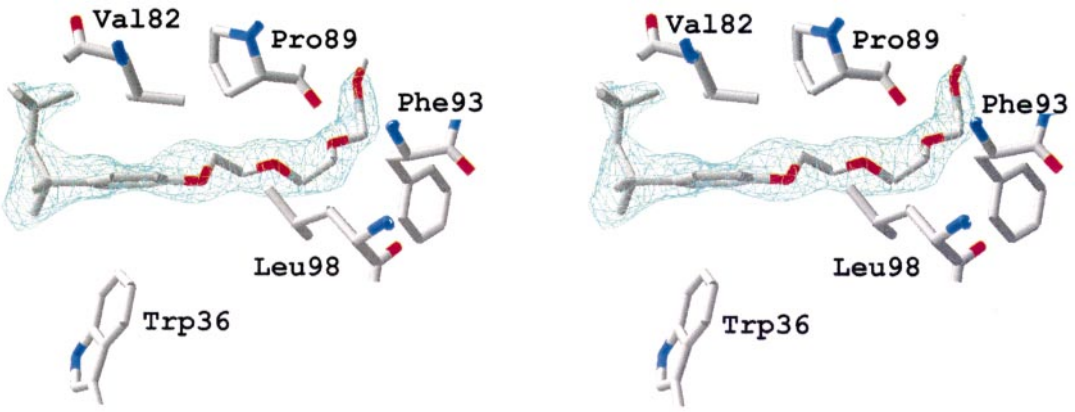

Figure 5. Electron-density of Triton X-100 as bound to dΔhΔSCP-2L. The Figure shows the electron density in the hydrophobic tunnel. The map is a weighted $2F_o - F_c$ map contoured at 0.8σ and calculated after refinement and without the Triton molecule included in the model. Phe93 and Leu98 form part of the entrance of the tunnel. The Figure was prepared with Swiss-PdbViewer.[30]

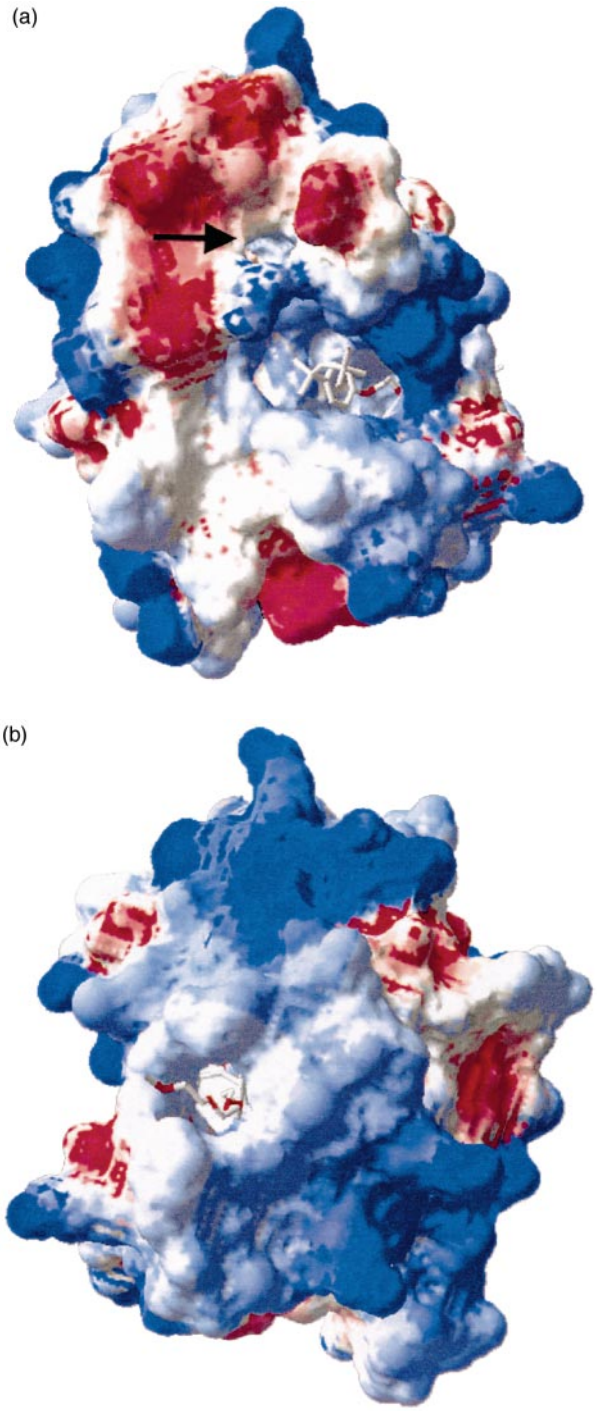

Figure 6. Electrostatic surface potential of the liganded dΔhΔSCP-2L structure. Negative surface potentials are marked with red, positive surface potentials with blue and neutral potentials with white. (a) Exit of the tunnel, showing the tetramethylbutyl-fragment of the ligand. There exists an extra hole, marked with an arrow, near the exit of the tunnel, which is not present in the rabbit SCP-2 crystal structure.[24] (b) Entrance of the tunnel, displaying the solvent-exposed ethoxy-repeat of the ligand. The Figures were produced with Swiss-PdbViewer.[30]

bile acid intermediates and straight-chain and branched-chain fatty acyl groups, all of which are known to be ligands of MFE-2.[10]

The entrance of the tunnel is formed by the amino acid residues Gln90, Phe93, Leu98, Ala100, Ile104, Met105 and Gln108 in the helices D and E and β-strand V (Figures 2 and 6(b)). Parts of the side of the tunnel between the helices D and E are composed of the polar amino acids Gln90, Gln108, Gln111 and Lys115, where the oxygen and nitrogen atoms of the side-chains form a hydrogen bonding network. Otherwise, the tunnel is lined by hydrophobic residues Phe12, Ile15, Phe34, Trp36, Trp48, Ile50, Ile72, Leu74, Phe79, Val82, Pro89 and Met112. The exit of the tunnel is formed by regions of helices A, C and E (Figures 2 and 6(a)). Even though the diameter of the exit is more than 10 Å, the amino acid residues Val11, Ile15, Trp36, Phe79 and Val83 in the proximity of the exit form a steric hindrance for the tetramethylbutyl part of the triton molecule, thus preventing it from completely using the space provided by the tunnel.

Close to the exit of the tunnel a side branch is observed, which reaches the surface of the protein in a relatively hydrophobic environment between the end of helices A and E (Figure 6(a)). Another cavity with a volume of 35 $Å^3$ is located between helices C and D. It is confined by the side-chains of residues Leu74, Asp78, Val82, Leu87, Ala92, Arg97 and Leu98, and the center of this cavity is only 5 Å apart from O34 of the triton molecule. The additional cavities suggest that molecules larger than Triton X-100 could bind in the tunnel.

Ligand-protein contacts

The contacts between Triton X-100 and dΔhΔSCP-2L were derived with LPC[34] and WHAT IF.[35] The octylphenol end and the three ethoxy repeats of the triton molecule interact with several apolar amino acid residues in the tunnel (Figure 4 and Table 1). All together, 59 contacts are formed between the protein and triton molecule using a cut-off distance of 4 Å. Most of the contacts are hydrophobic or aromatic; only one hydrogen bond is formed by the NE2 of Gln108 and O55 of the triton molecule. More van der Waals interactions exist around the ethoxy repeats than around the octylphenol end. Of particular note is Gln108, near the entrance of the tunnel, which interacts strongly with the C52, O55 and C58 of the Triton X-100 (Table 1).

Discussion

The structure of dΔhΔSCP-2L complexed with Triton X-100 presented here demonstrates a hydrophobic tunnel that traverses the protein molecule and accommodates the bound ligand. The importance of apolar interactions for binding in the tunnel agrees with the results previously obtained by fluorescence resonance energy transfer measurements, which indicated an ordered binding pocket

Table 1. Contact distances between Triton X-100 and dΔhΔSCP-2L

Triton X-100	dΔhΔSCP-2L	Contact distance (Å)
C4	Val83, CA	4.0
C4	Val83, CG2	4.0
C5	Gln111, CG	3.9
C5	Lys115, NZ	4.0
C18	Trp36, CH2	3.6
C19	Phe79, CE2	3.7
C19	Phe79, CZ	3.8
C19	Val83, CG2	3.9
C20	Trp36, CZ2	4.0
C20	Trp36, CH2	4.0
C20	Leu114, CD1	3.7
C27	Trp36, CH2	3.7
C27	Val82, CG1	3.8
C28	Trp36, CH2	3.9
C28	Val82, CG1	3.9
C29	Trp36, CH2	4.0
C30	Trp36, CH2	3.9
C30	Gln111,CB	3.9
C30	Ser107, O	3.5
C31	Trp36, CH2	3.7
O34	Pro89, CB	3.9
C37	Pro89, CB	3.7
C37	Gln90, NE2	3.8
C37	Ser107, O	3.8
C37	Gln111, OE1	3.2
C38	Gln90, NE2	3.6
C38	Ser107, C	3.7
C38	Ser107, O	3.8
C38	Ser107, CB	3.6
C38	Ser107, OG	3.2
C38	Gln108, N	3.8
C38	Gln111, OE1	3.8
O41	Gln90, NE2	3.2
O41	Ser107, OG	3.9
C44	Ser107, OG	3.5
C45	Gln90, NE2	3.9
C45	Phe93, CB	3.6
C45	Phe93, CG	3.6
C45	Phe93, CD1	4.0
C45	Phe93, CD2	4.0
O48	Gln90, CG	4.0
O48	Gln90, NE2	3.6
O48	Gln108, CD	4.0
O48	Gln108, OE1	3.8
C51	Phe93, CD2	4.0
C51	GIn108, OE1	4.0
C52	Met105, SD	3.5
C52	Gln108, CD	3.7
C52	Gln108, OE1	3.0
C52	Gln108, NE2	3.8
O55	Gln90, CG	3.1
O55	Phe94, CE2	3.9
O55	Gln108, CD	3.4
O55	Gln108, OE1	3.0
O55	Gln108, NE2	3.1
C58	Gln90, CG	4.0
C58	Gln108, CD	3.7
C58	Gln108, OE1	3.2
C58	Gln108, NE2	3.4

The schematic drawing of Triton X-100 and the amino acid residues involved in the contacts is shown in Figure 4. The ligand protein contacts were analyzed with LPC[34] and WHAT IF.[35]

in the human SCP-2 strongly interacting with fatty acyl-CoA (K_d of 2-4 nM).[36,37] The hydrophobic tunnel was also described in the unliganded rabbit SCP-2 crystal structure[24] and the authors hypothesized the putative entrance and the exit of the tunnel. In the dΔhΔSCP-2L the Triton X-100 enters the tunnel through the entrance surrounded by helices D and E and β-strand V. Interestingly, this region is highly conserved in the SCP-2 family (Figure 1) and it is tempting to speculate that this conservation reflects functional similarity within this family. Compared to rabbit SCP-2, the length of the tunnel in the liganded dΔhΔSCP-2L is the same, yet it is somewhat wider. Moreover, regions near the tunnel, such as the loop between β-strands I and II and the C-terminal helix, have moved relative to their positions in the unliganded rabbit SCP-2 structure, indicating conformational changes upon ligand binding (Figure 3).

The highest affinity ligands for human SCP-2 are acyl-CoAs of carbon chain length of 24 and 26 with or without a double bond at the second position.[36,37] Surface plasmon resonance binding experiments of various fatty acyl-CoAs and dΔhΔSCP-2L were done, such that dΔhΔSCP-2L was coupled onto the surface and acyl-CoA esters were flushed over. These experiments demonstrated binding between dΔhΔSCP-2L and fatty acyl-CoA esters, with long and very-long-chain acyl-CoA esters being the best ligands (P.P., A.M.H., L. Hirvelä, J.K.H. & T.G., unpublished results). Unfortunately, attempts to incorporate these ligands into the crystals of dΔhΔSCP-2L have so far failed. The positively charged cluster (Arg97-Arg101) near the entrance of the tunnel in dΔhΔSCP-2L could provide an interaction site for the pyrophosphate groups of the CoA molecule. If the pantetheine group of CoA enters the tunnel in dΔhΔSCP-2L, the remaining length of the tunnel will cover the fatty acyl part of only up to eight carbon atoms. Consequently, the ω-end of a bound acyl group longer than this will protrude out of the tunnel. The hydrophobic face of dΔhΔSCP-2L, which also contains the exit of the tunnel (Figure 6(a)), is the potential interaction site with the hydratase 2 domain in wild-type MFE-2. This interface could provide a hydrophobic environment for the longer fatty acyl tails. Such a mode of binding is also observed in 2-enoyl-CoA hydratase 1.[38] In this structure a bound fatty acyl-CoA shorter than C6 occupies the whole of the binding pocket. However, the ω-end of the longer fatty acid group enters a hydrophobic region between subunits in the enzyme, which is revealed when a flexible loop at the bottom of the active site moves aside.

Peroxisomal matrix proteins are folded in the cytosol and subsequently imported into peroxisomes *via* a receptor-mediated transport system.[39,40] In the case of peroxisomal targeting signal type 1 (PTS1), the C-terminal signaling peptide interacts with the soluble receptor protein, Pex5p; subsequently, the Pex5p-cargo protein complex interacts with docking proteins at the peroxisome membrane. So far, a number of structures of proteins containing the PTS1 have been reported (see for example PDB entries 1gga, 1gyp, 1lci, 1kif, 1gox, 1a7k, 1dci, 1qnd and 1c44), but only in 1dci

(dienoyl-CoA isomerase)[41] and 1c44 (SCP-2)[24] the structure of PTS1 is defined. In the hexameric dienoyl-CoA isomerase PTS1 is bound in a pocket between the two trimers; both hydrophobic interactions and hydrogen-bonding interactions stabilize the structure of the signaling peptide, and the PTS1 adopts an extended, buried conformation. In the crystal structure of unliganded rabbit SCP-2 the PTS1 peptide is also ordered but bound to the surface of the bulk of the protein;[24] the NMR structure of the human SCP-2 indicates a high degree of disorder for this peptide segment.[25] The liganded structure described here shows that the C-terminal residues have adopted a very different conformation (as compared to the unliganded rabbit SCP-2), such that helix E now continues to the C terminus itself (Figure 3). The structural differences also extend towards the N terminus of helix E, where a smaller ligand-induced conformational switch is observed. This rearrangement agrees with the observation that the human variants N104D and N104I have decreased affinity for the ligand.[42] In addition, in the liganded dΔhΔSCP-2L structure, the C-terminal AKL peptide is ordered and fully solvent exposed, thus being able to interact with a receptor molecule of the peroxisomal import system. These observations support the hypothesis[24,25] about ligand assisted protein import into peroxisomes.

Materials and Methods

Strains

All bacterial manipulations were performed with *E. coli* strain DH5α.

Construction of plasmid *pET3d::dΔhΔSCP-2L*

Standard molecular biology methods were performed according to procedures by Sambrook and co-workers.[43] The open reading frame of human *MFE-2* cDNA was obtained from total RNA isolated from human fibroblasts[44] by reverse transcription with Moloney murine leukemia virus reverse transcriptase (Life Technologies Inc.) and amplified by PCR using human *MFE-2*-specific primers: 5′-primer cacttccatg GAG GGC GGG AAG CTT CAG AGT and 3′-primer cacctggatcc TCA GAG CTT GGC GTA GTC TTT AA (lower case sequences indicate mismatches to the human *MFE-2* cDNA sequence). The PCR-product was subsequently subcloned into pUC18 vector using the Sure Clone Ligation kit (Amersham Pharmacia Biotech AB) and the nucleotide sequence encoding the C-terminal domain of human MFE-2, *dΔhΔSCP-2L*, was verified. The embedded *Nco*I and *Bam*HI restriction endonuclease sites in the PCR primers (underlined) allowed the release of a 369 bp insert and subsequent cloning into pET-3d expression vector (Novagen) yielding the plasmid *pET3d::dΔhΔSCP-2L*. This plasmid was used for expression in *E. coli* BL21(DE3) pLysS cells.

Protein expression and purification

M9ZB medium supplemented with 50 μg/ml carbenicillin and 34 μg/ml chloramphenicol was used for expression experiments. A 10 ml portion of an overnight culture of *E. coli* cells containing the plasmid *pET3d::dΔhΔSCP-2L* was used to inoculate one liter of culture. The cells were allowed to grow at 37 °C under aerobic conditions until A_{600} of 0.6 was reached. The expression of recombinant protein was induced by the addition of isopropyl-1-thio-β-D-galactopyranoside (IPTG) to a final concentration of 0.4 mM. After two hours of additional incubation at 37 °C the bacterial cells were harvested, washed with the cold buffer (120 mM NaCl, 16 mM potassium phosphate, pH 7.4, 0.02% NaN_3) and stored at −70 °C until used.

A bacterial cell pellet (3.5 g wet weight) was suspended in 50 ml of 20 mM 3-(cyclohexylamino)-1-propanesulfonic acid (CAPS), 0.5 mM benzamidine hydrochloride hydrate (BA), pH 11.0 (buffer A), containing 100 μg/ml lysozyme, 25 μg/ml DNase I, 25 μg/ml RNase A and 10 mM $MgCl_2$. Cell fractions from broken bacterial cells were collected by centrifugation (33,000 ***g***, 45 minutes, 4 °C), and the supernatant was applied to an anion exchange Q Sepharose column (2.5 cm × 13 cm, Amersham Pharmacia Biotech AB) equilibrated with buffer A. The bound proteins were eluted with a 600 ml linear gradient of 35 mM to 600 mM NaCl. The pooled Q Sepharose fractions containing dΔhΔSCP-2L were dialyzed against buffer B (20 mM 2-(*N*-morpholino)ethanesulfonic acid (MES), 35 mM NaCl, pH 6.0) and applied to a cation exchange Resource S (6.0 ml, Amersham Pharmacia Biotech AB) column equilibrated with the buffer B. The bound proteins were eluted in a NaCl gradient increasing linearly from 35 mM to 100 mM for 60 minutes at a flow rate of 2.0 ml/minute. Peak fractions consisting of dΔhΔSCP-2L were pooled, concentrated and applied to a size exclusion chromatography column Superdex™ 75 HR 10/30 (Amersham Pharmacia Biotech AB) column equilibrated with buffer C (20 mM piperazine-*N*,*N*′-bis(2-ethanesulfonic acid) (Pipes), 1 mM ethylene diaminetetraacetic acid (EDTA), 1 mM sodium azide (NaN_3), 150 mM NaCl, pH 7.5). Proteins were eluted at a flow rate of 250 μl/minute. The protein purification was monitored by SDS-PAGE. Mass spectrometric analyses and N-terminal sequencing were performed on the recombinant protein to confirm the identity of the dΔhΔSCP-2L.

Crystallization of dΔhΔSCP-2L

The dΔhΔSCP-2L -protein sample obtained from the Superdex column was concentrated to 2.7 mg/ml by centrifugal filtration and Triton X-100 (Riedel-de-Haën, product number 56029) was added to a final concentration of 0.23 mM. Originally, Triton X-100 was used to increase the solubility to higher protein concentrations. Later on, it was noticed that triton molecule not only enhanced the solubility but also was critical to crystallization; when Triton X-100 was removed from the protein sample, no crystals were obtained. Initial crystallization screening was performed by the sparse matrix screening method described by Jancarik & Kim.[45] Crystals were grown at 4 °C using the hanging-drop vapor-diffusion method. The optimized precipitant solution contained 2.30 M ammonium sulfate, 100 mM citric acid (pH 5.6), 200 mM NaCl. Trigonal prismatic shaped crystals grown under these conditions reached a size of up to 0.25 mm × 0.20 mm × 0.40 mm in about ten days.

Data collection and processing

The dΔhΔSCP-2L crystal was transferred to cryoprotecting mother liquor that was made by adding sucrose to the original mother liquor to a final concentration of 25 % (w/v). Sucrose was allowed to diffuse into the crystal for 30 minutes before the crystal was flash frozen at 100 K. Data were collected by the oscillation method with 0.5° rotations per frame at a wavelength of 0.9785 Å using a MAR CCD detector at beamline BW7A at the EMBL outstation at the DESY synchrotron, Hamburg, Germany. A data set, with R_{sym} of 0.031, was collected to 1.75 Å resolution. Images were processed using DENZO and reflections merged using SCALEPACK of the HKL suite.[46] The final statistics for the processing of the native dataset is given in Table 2. The dΔhΔSCP-2L crystal belonged to the orthorhombic space group $P2_12_12_1$ with unit cell dimensions of $a = 35.47$ Å, $b = 50.03$ Å, $c = 62.73$ Å and $\alpha, \beta, \gamma = 90°$. The assumption of one molecule per asymmetric unit was made based on Matthews coefficient value[47] of 2.10 Å^3/Da which also indicates the solvent content to be 41 %.

Table 2. Data collection, refinement statistics and quality of the model

Data set	dΔhΔSCP-2L + Triton X-100
A. *Data collection statistics*	
Space group	$P2_12_12_1$
Unit cell parameters	
a (Å)	35.474
b (Å)	50.028
c (Å)	62.725
Temperature (K)	100
Wavelength (Å)	0.9785
Resolution (Å)	20-1.75 (1.81-1.75)
R_{merge} (%)[b]	3.1 (25.9)
Completeness (%)	98.3 (97.1)
$I/\sigma I$	27.7 (3.4)
Unique reflections	11,659 (1132)
Redundancy	3.6
Mosaicity (deg.)	0.9
B-factor from Wilson plot (Å^2)	26
B. *Refinement statistics*	
Resolution (Å)	18.0-1.75
Total number of reflections	11,554
Working set: number of reflections	11,059
R_{factor} (%)	19.2
Test set: number of reflections	495
R_{free} (%)	21.4
Protein atoms	898
Water atoms	125
Sulfate atoms	10
Triton X-100 atoms	25
C. *Geometry statistics*	
rmsd bond distance) (Å)	0.010
rmsd (bond angle) (deg.)	1.51
rmsd B	
Main-chain bonded atoms (Å^2)	1.51
Side-chain bonded atoms (Å^2)	2.09
Average *B*-factor	
All atoms (Å^2)	30.3
Main-chain atoms (Å^2)	28.8
Side-chain atoms (Å^2)	31.9
Water molecules (Å^2)	44.7
Triton X-100 (Å^2)	46.7
Ramachandran plot[c]	
Most favored region (%)	92.9
Additionally allowed regions (%)	7.1
Generously allowed regions (%)	0
Disallowed regions (%)	0

[a] The values in parentheses are for the highest resolution shell.
[b] $R_{merge} = \Sigma_h \Sigma_i |I - I_i| / \Sigma_h \Sigma_i I_i$.
[c] As defined by PROCHECK.

Structure determination, model building and refinement

Molecular replacement was employed for the structure determination. Initial phases were determined from a molecular replacement solution obtained with AMoRe[48] using the rabbit SCP-2[24] (PDB entry 1c44) as the search model. The successful molecular replacement calculations were done with a model in which the regions of high sequence variability, amino acids 1-11 and 113-123 and the loop between β-strands III and IV, were removed from the reference model. Molecular replacement gave one solution that stood out from the others with the correlation coefficient of 28.6 % ($R = 50.9$ %) after rigid body refinement. Application of the spacegroup symmetry resulted in reasonable packing. The refinement was started with a simulated annealing run using CNS.[49] Of the diffraction data, 4.2 % were used for cross-validation. After simulated annealing ($R = 42.8$ %, $R_{free} = 48.5$ %), changing amino acids to correspond dΔhΔSCP-2L sequence, XYZ and *B*-factors refinements and using all the data to 1.75 Å, the *R*-factor decreased to 36.2 % ($R_{free} = 39.5$ %). The phases were then used as input for the autobuilding procedure in warpNtrace.[50] After 200 cycles of building and refinement, 101 of the 120 residues in the asymmetric unit were built. Using the side-chain building algorithm in warpNtrace, side-chains for all these residues were built. This structure was then used as a starting point for further refinement and model building using CNS. Water molecules were added to the model where the difference density exceeded 3σ and the peaks were within a reasonable distance to hydrogen bonding partners on the protein (<3.6 Å). While adding water molecules, the triton molecule that was bound to protein was included in the refinement steps, as well. The resulting final model has an *R*-factor of 19.2 % ($R_{free} = 21.4$ %) using data between 18 and 1.75 Å, with good stereochemistry (Table 2) and continuous density for the backbone from residues 6 to 120 (Leu622-Leu736 in the wild-type human MFE-2). The quality of the model was assessed with the structure-validation programs PROCHECK[51] and WHAT IF.[35] A total of 92.9 % of the amino acid residues lie within the most favored regions of the Ramachandran plot. The remaining residues (7.1 %) are located within the additionally allowed region.

Identification of the ligand, Triton X-100

To identify the ligand, Triton X-100, within dΔhΔSCP-2L, mass spectrometric analyses were carried out for the purified dΔhΔSCP-2L, Triton X-100 and the crystal. Before measurements the crystal was washed a few times with mother liquor without Triton X-100 and then transferred to water. The experiments were performed using a LCT (Micromass LTD) orthogonal time-of-flight mass spectrometer with OpenLynx3 Data

system. The diluted samples in acetonitrile-water solution (50:50) containing 0.1 % formic acid solution were directed by a Harward 5311 syringe pump into the Z-spray electrospray source at a flow rate of 10 μl/minute. The vaporizer temperature was 140 °C and N_2 was used both as nebulizer (80 l/hour) gas and desolvation (400 l/hour) gas. The electrospray capillary was kept at 3.8 kV and the sample cone voltage at 35 V.

Construction of topology and parameter files for Triton X-100

Our study describes for the first time the crystallographic structure of Triton X-100 bound to a protein. For this reason, the topology and parameter files of Triton X-100 for the refinement cycles had to be created. Interatomic bonding distances and angles for the (1,1,3,3-tetramethyl)butyl part of triton molecule (Figure 4) were obtained from the study on the 1-(1,1,3,3-tetramethyl)butyl-4-phenyl-1,2,4-triazoline-3,5-dione crystal structure by Baker and co-workers.[52] For the phenyl ring and its adjacent carbon and oxygen atoms the available information from a tyrosine side-chain was applied. For the bond distances and angles of the ethoxy repeat (carbon-carbon-oxygen repeat), carbohydrate parameters, provided by the CNS program, were taken into account.

Surface plasmon resonance measurements

dΔhΔSCP-2L protein was immobilized on a carboxymethylated dextran matrix (CM5) chip with standard amine coupling chemistry by flowing a solution of 11.6 μg/ml protein in 10 mM potassium phosphate buffer (pH 4.8), at the flow rate of 5 μl/minute for seven minutes over the chip in a Biacore® 3000 instrument (Biacore AB, Uppsala, Sweden). The amount of immobilized dΔhΔSCP-2L was 1900 resonance units. Aralytes were flushed over the chip in 100 mM potassium phosphate buffer, pH 5.5 or 7.0, with a flow rate of 40 μl/minute. K_d values were estimated with the steady state affinity model according to the manufacturer's procedure implemented in BIA evaluation 3.1.

Protein Data Bank accession number

The coordinates and structure factors of the liganded structure (1IKT) have been deposited at the RCSB.

Acknowledgments

This work was supported by grants from the Academy of Finland and the Sigrid Jusélius Foundation (to J.K.H.) and Wellcome Trust Career Development Research Fellowship (to D.M.F. v. A.). We acknowledge the EMBL Hamburg Outstation for the opportunity to collect data at the DESY synchrotron beamline BW7A, especially Dr Paul Tucker. We thank Dr Klaus Piontek for giving access to coordinate data prior to release, Dr Lloyd Ruddock for critical comments on the manuscript and Eeva-Liisa Stefanius for excellent technical assistance.

References

1. Hiltunen, J. K., Filppula, S. A., Koivuranta, K. T., Siivari, K., Qin, Y. M. & Häyrinen, H. M. (1996). Peroxisomal β-oxidation and polyunsaturated fatty acids. *Ann. NY Acad. Sci.* **804**, 116-128.
2. Jiang, L. L., Miyazawa, S., Souri, M. & Hashimoto, T. (1997). Structure of D-3-hydroxyacyl-CoA dehydratase/D-3-hydroxyacyl-CoA dehydrogenase bifunctional protein. *J. Biochem.* **121**, 364-369.
3. Leenders, F., Adamski, J., Husen, B., Thole, H. H. & Jungblut, P. W. (1994). Molecular cloning and amino acid sequence of the porcine 17 β-estradiol dehydrogenase. *Eur. J. Biochem.* **222**, 221-227.
4. Jiang, L. L., Kobayashi, A., Matsuura, H., Fukushima, H. & Hashimoto, T. (1996). Purification and properties of human D-3-hydroxyacyl-CoA dehydratase: medium-chain enoyl-CoA hydratase is D-3-hydroxyacyl-CoA dehydratase. *J. Biochem.* **120**, 624-632.
5. Hiltunen, J. K. & Qin, Y. (2000). β-Oxidation - strategies for the metabolism of a wide variety of acyl-CoA esters. *Biochim. Biophys. Acta,* **1484**, 117-128.
6. Dieuaide-Noubhani, M., Novikov, D., Baumgart, E., Vanhooren, J. C., Fransen, M., Goethals, M. *et al.* (1996). Further characterization of the peroxisomal 3-hydroxyacyl-CoA dehydrogenases from rat liver. Relationship between the different dehydrogenases and evidence that fatty acids and the C27 bile acids di- and tri-hydroxycoprostanic acids are metabolized by separate multifunctional proteins. *Eur. J. Biochem.* **240**, 660-666.
7. Qin, Y. M., Poutanen, M. H., Helander, H. M., Kvist, A. P., Siivari, K. M., Schmitz, W. *et al.* (1997). Peroxisomal multifunctional enzyme of β-oxidation metabolizing D-3-hydroxyacyl-CoA esters in rat liver: molecular cloning, expression and characterization. *Biochem. J.* **321**, 21-28.
8. Leenders, F., Tesdorpf, J. G., Markus, M., Engel, T., Seedorf, U. & Adamski, J. (1996). Porcine 80-kDa protein reveals intrinsic 17β-hydroxysteroid dehydrogenase, fatty acyl-CoA-hydratase/dehydrogenase, and sterol transfer activities. *J. Biol. Chem.* **271**, 5438-5442.
9. de Launoit, Y. & Adamski, J. (1999). Unique multifunctional HSD17B4 gene product: 17β-hydroxysteroid dehydrogenase 4 and D-3-hydroxyacyl-coenzyme A dehydrogenase/hydratase involved in Zellweger syndrome. *J. Mol. Endocrinol.* **22**, 227-240.
10. Baes, M., Huyghe, S., Carmeliet, P., Declercq, P. E., Collen, D., Mannaerts, G. P. & van Veldhoven, P. P. (2000). Inactivation of the peroxisomal multifunctional protein-2 in mice impedes the degradation of not only 2-methyl-branched fatty acids and bile acid intermediates but also of very long chain fatty acids. *J. Biol. Chem.* **275**, 16329-16336.
11. Hiltunen, J. K., Wenzel, B., Beyer, A., Erdmann, R., Fosså, A. & Kunau, W. H. (1992). Peroxisomal multifunctional β-oxidation protein of *Saccharomyces cerevisiae*. Molecular analysis of the fox2 gene and gene product. *J. Biol. Chem.* **267**, 6646-6653.
12. Qin, Y. M., Haapalainen, A. M., Conry, D., Cuebas, D. A., Hiltunen, J. K. & Novikov, D. K. (1997). Recombinant 2-enoyl-CoA hydratase derived from rat peroxisomal multifunctional enzyme 2: role of the hydratase reaction in bile acid synthesis. *Biochem. J.* **328**, 377-382.

13. Barnes, T. M., Jin, Y., Horvitz, H. R., Ruvkun, G. & Hekimi, S. (1996). The *Caenorhabditis elegans* behavioral gene unc-24 encodes a novel bipartite protein similar to both erythrocyte band 7.2 (stomatin) and nonspecific lipid transfer protein. *J. Neurochem.* **67**, 46-57.
14. Tan, H., Okazaki, K., Kubota, I., Kamiryo, T. & Utiyama, H. (1990). A novel peroxisomal nonspecific lipid-transfer protein from *Candida tropicalis*. Gene structure, purification and possible role in β-oxidation. *Eur. J. Biochem.* **190**, 107-112.
15. Seidel, G. & Prohaska, R. (1998). Molecular cloning of hSLP-1, a novel human brain-specific member of the band 7/MEC-2 family similar to *Caenorhabditis elegans* UNC-24. *Gene,* **225**, 23-29.
16. Subramani, S. (1996). Protein translocation into peroxisomes. *J. Biol. Chem.* **271**, 32483-32486.
17. Erdmann, R. & Blobel, G. (1996). Identification of Pex13p a peroxisomal membrane receptor for the PTS1 recognition factor. *J Cell. Biol.* **135**, 111-121.
18. Ohba, T., Rennert, H., Pfeifer, S. M., He, Z., Yamamoto, R. & Holt, J. A., *et al*. (1994). The structure of the human sterol carrier protein X/sterol carrier protein 2 gene (SCP2). *Genomics,* **24**, 370-374.
19. Leenders, F., Dolez, V., Begue, A., Moller, G., Gloeckner, J. C., de Launoit, Y. & Adamski, J. (1998). Structure of the gene for the human 17β-hydroxysteroid dehydrogenase type IV. *Mamm. Genome,* **9**, 1036-1041.
20. Seedorf, U., Raabe, M., Ellinghaus, P., Kannenberg, F., Fobker, M., Engel, T. *et al*. (1998). Defective peroxisomal catabolism of branched fatty acyl coenzyme A in mice lacking the sterol carrier protein-2/sterol carrier protein-x gene function. *Genes Dev.* **12**, 1189-1201.
21. Pfeifer, S. M., Furth, E. E., Ohba, T., Chang, Y. J., Rennert, H., Sakuragi, N. *et al*. (1993). Sterol carrier protein 2: a role in steroid hormone synthesis?. *J. Steroid. Biochem. Mol. Biol.* **47**, 167-172.
22. Puglielli, L., Rigotti, A., Greco, A. V., Santos, M. J. & Nervi, F. (1995). Sterol carrier protein-2 is involved in cholesterol transfer from the endoplasmic reticulum to the plasma membrane in human fibroblasts. *J. Biol. Chem.* **270**, 18723-18726.
23. Wouters, F. S., Bastiaens, P. I., Wirtz, K. W. & Jovin, T. M. (1998). FRET microscopy demonstrates molecular association of non-specific lipid transfer protein (nsL-TP) with fatty acid oxidation enzymes in peroxisomes. *EMBO J.* **17**, 7179-7189.
24. Choinowski, T., Hauser, H. & Piontek, K. (2000). Structure of sterol carrier protein 2 at 1.8 Å resolution reveals a hydrophobic tunnel suitable for lipid binding. *Biochemistry,* **39**, 1897-1902.
25. Garcia, F. L., Szyperski, T., Dyer, J. H., Choinowski, T., Seedorf, U., Hauser, H. & Wüthrich, K. (2000). NMR structure of the sterol carrier protein-2: implications for the biological role. *J. Mol. Biol.* **295**, 595-603.
26. Altschul, S. F., Madden, T. L., Schaffer, A. A., Zhang, J., Zhang, Z., Miller, W. & Lipman, D. J. (1997). Gapped BLAST and PSI-BLAST: a new generation of protein database search programs. *Nucl. Acids Res.* **25**, 3389-3402.
27. Thompson, J. D., Higgins, D. G. & Gibson, T. J. (1994). CLUSTAL W: improving the sensitivity of progressive multiple sequence alignment through sequence weighting, positions-specific gap penalties and weight matrix choice. *Nucl. Acids Res.* **22**, 4673-4680.
28. Requena, N., Füller, P. & Franken, P. (1999). Molecular characterization of GmFOX2, an evolutionarily highly conserved gene from the mycorrhizal fungus *Glomus mosseae*, down-regulated during interaction with rhizobacteria. *Mol. Plant Microbe Interact.* **12**, 934-942.
29. Kabsch, W. & Sander, C. (1983). Dictionary of protein secondary structure: pattern recognition of hydrogen-bonded and geometrical features. *Biopolymers,* **22**, 2577-2637.
30. Guex, N. & Peitsch, M. C. (1997). SWISS-MODEL and the Swiss-PdbViewer: an environment for comparative protein modeling. *Electrophoresis,* **18**, 2714-2723.
31. Lerche, M. H., Kragelund, B. B., Bech, L. M. & Poulsen, F. M. (1997). Barley lipid-transfer protein complexed with palmitoyl CoA: the structure reveals a hydrophobic binding site that can expand to fit both large and small lipid-like ligands. *Structure,* **5**, 291-306.
32. van Aalten, D. M., DiRusso, C. C., Knudsen, J. & Wierenga, R. K. (2000). Crystal structure of FadR, a fatty acid-responsive transcription factor with a novel acyl coenzyme A-binding fold. *EMBO J.* **19**, 5167-5177.
33. Andersen, K. V. & Poulsen, F. M. (1993). The three-dimensional structure of acyl-coenzyme A binding protein from bovine liver: structural refinement using heteronuclear multidimensional NMR spectroscopy. *J. Biomol. NMR,* **3**, 271-284.
34. Sobolev, V., Sorokine, A., Prilusky, J., Abola, E. E. & Edelman, M. (1999). Automated analysis of interatomic contacts in proteins. *Bioinformatics,* **15**, 327-332.
35. Vriend, G. (1990). WHAT IF: a molecular modeling and drug design program. *J. Mol. Graph.* **8**, 52-56.
36. Dansen, T. B., Westerman, J., Wouters, F. S., Wanders, R. J., van Hoek, A., Gadella, T. W., Jr & Wirtz, K. W. (1999). High-affinity binding of very-long-chain fatty acyl-CoA esters to the peroxisomal non-specific lipid-transfer protein (sterol carrier protein-2). *Biochem. J.* **339**, 193-199.
37. Frolov, A., Cho, T. H., Billheimer, J. T. & Schroeder, F. (1996). Sterol carrier protein-2, a new fatty acyl coenzyme A-binding protein. *J. Biol. Chem.* **271**, 31878-31884.
38. Engel, C. K., Kiema, T. R., Hiltunen, J. K. & Wierenga, R. K. (1998). The crystal structure of enoyl-CoA hydratase complexed with octanoyl-CoA reveals the structural adaptations required for binding of a long chain fatty acid-CoA molecule. *J. Mol. Biol.* **275**, 847-859.
39. Elgersma, Y., Kwast, L., Klein, A., Voorn-Brouwer, T., van den Berg, M., Metzig, B. *et al*. (1996). The SH3 domain of the *Saccharomyces cerevisiae* peroxisomal membrane protein Pex13p functions as a docking site for Pex5p, a mobile receptor for the import PTS1-containing proteins. *J. Cell Biol.* **135**, 97-109.
40. Albertini, M., Rehling, P., Erdmann, R., Girzalsky, W., Kiel, J. A., Veenhuis, M. & Kunau, W. H. (1997). Pex14p, a peroxisomal membrane protein binding both receptors of the two PTS-dependent import pathways. *Cell,* **89**, 83-92.
41. Modis, Y., Filppula, S. A., Novikov, D. K., Norledge, B., Hiltunen, J. K. & Wierenga, R. K. (1998). The crystal structure of dienoyl-CoA isomerase at 1.5 Å resolution reveals the importance of aspartate and

glutamate sidechains for catalysis. *Structure,* **15**, 957-970.
42. Seedorf, U., Scheek, S., Engel, T., Steif, C., Hinz, H. J. & Assmann, G. (1994). Structure-activity studies of human sterol carrier protein 2. *J. Biol. Chem.* **269**, 2613-2618.
43. Sambrook, J., Fritzch, E. F. & Maniatis, T. (1989). *Molecular Cloning: A Laboratory Manual*, Cold Spring Harbor Laboratory Press, Cold Spring Harbor, NY.
44. Chomczynski, P. & Sacchi, N. (1987). Single-step method of RNA isolation by acid guanidinium thiocyanate-phenol-chloroform extraction. *Anal. Biochem.* **162**, 156-159.
45. Jancarik, J. & Kim, S.-H. (1991). Sparse matrix sampling: screening method for crystallization of proteins. *J. Appl. Crystallog.* **24**, 409-411.
46. Otwinowski, Z. & Minor, W. (1997). Processing of X-ray diffraction data collected in oscillation mode. *Methods Enzymol.* **276**, 307-326.
47. Matthews, B. W. (1968). Solvent content of crystals. *J. Mol. Biol.* **33**, 491-497.
48. Nawaza, J. (1994). AMoRe: an automated package for molecular replacement. *Acta Crystallog. sect. A,* **50**, 157-163.
49. Brünger, A. T. (1998). Crystallography & NMR system: a new software system for macromolecular structure determination. *Acta Crystallog. sect. D,* **54**, 905-921.
50. Perrakis, A., Morris, R. & Lamzin, V. S. (1999). Automated protein model building combined with iterative structure refinement. *Nature Struct. Biol.* **6**, 458-463.
51. Laskowski, R. A., McArthur, M. W., Moss, D. S. & Thornton, J. M. (1993). PROCHECK: a program to check the stereochemical quality of protein structures. *J. Appl. Crystallog.* **26**, 283-291.
52. Baker, R. J., Timberlake, J. W., Alender, J. T., Majeste, R. J. & Trefonas, L. M. (1982). 1-(1,1,3,3-tetramethyl)butyl-4phenyl-1,2,4-triazoline-3,5-dione. *Cryst. Struct. Commun.* **11**, 763-768.

Edited by R. Huber

(Received 22 May 2001; received in revised form 10 September 2001; accepted 17 September 2001)